Journal of Microbiology (2015) Vol. 53, No. 4, pp. 243–249
DOI 10.1007/s12275-015-5067-7

Multiple roles of a putative vacuolar protein sorting associated protein 74, FgVPS74, in the cereal pathogen *Fusarium graminearum*

Hee-Kyoung Kim[1], Ki Woo Kim[2], and Sung-Hwan Yun[1]*

[1]*Department of Medical Biotechnology, Soonchunhyang University, Asan 336-745, Republic of Korea*
[2]*School of Ecology & Environmental System, Kyungpook National University, Sangju 742-711, Republic of Korea*

(Received Feb 3, 2015 / Revised Feb 11, 2015 / Accepted Feb 11, 2015)

***Fusarium graminearum*, a member of the *F. graminearum* species complex, is a filamentous ascomycetous group that causes serious diseases in cereal crops. A screen of insertional mutants of *F. graminearum*, generated using a restriction enzyme-mediated integration method, identified a mutant designated R7048 showing pleiotropic phenotypes in several mycological traits. The vector insertion site in the R7048 genome was identified as the *Kpn*I site within an ORF annotated as FGSG_06346 (designated *FgVPS74*), which showed similarity to vacuolar protein sorting-associated protein 74 in the baker yeast. Both targeted gene deletion and complementation analyses confirmed that *FgVPS74* was involved in hyphal growth, conidiation, sexual development, mycotoxin production, and virulence towards host plants in *F. graminearum*. Electron microscopy analysis revealed no significant changes in morphology of the vacuole or other organelles, but a greater number of mitochondria were produced in the Δ*FgVPS74* strain compared to the wild-type progenitor. Expression of a GFP-tagged FgVPS74 construct under its native promoter in the Δ*FgVPS74* strain exhibited localization of GFP signal to putative vesicle structures, but not to the vacuolar membrane. Taken together, these findings demonstrated that a functional vacuolar protein-sorting pathway mediated by FgVPS74 is crucial for fungal growth and development in *F. graminearum*.**

***Keywords*:** vacuolar protein sorting-associated protein 74, *Fusarium graminearum*, hyphal growth, virulence, conidiation

Introduction

The fungal vacuole plays various roles in macromolecular degradation and other cellular processes such as metabolite storage, osmoregulation, and pH homeostasis, which are crucial for fungal growth, development, symbiosis, and pathogenesis (Veses *et al.*, 2008). Most proteins destined for vacuoles transit from the endoplasmic reticulum (ER) to the Golgi complex together with secretory proteins, and are sorted from other secretory traffic in the late Golgi compartment by a sorting apparatus for specific delivery to the vacuole. In the yeast *Saccharomyces cerevisiae*, the protein-sorting processes are performed through coordinated actions of various vacuolar protein sorting (*VPS*) genes that have been identified by both classical genetics and genomics approaches (Robinson *et al.*, 1988; Rothman *et al.*, 1989; Raymond *et al.*, 1992; Conibear and Stevens, 1995; Bonangelino *et al.*, 2002; Veses *et al.*, 2008). To date, more than 140 *VPS* genes have been characterized using the original *VPS* mutants, which were grouped into six classes (A through F) based on distinct vacuolar morphology defects (Raymond *et al.*, 1992) and genome-wide deletion mutants defective in the vacuolar protein-sorting process (Bonangelino *et al.*, 2002).

Since protein trafficking and sorting pathways are fundamental processes conserved in eukaryotes, homologs of several *VPS* genes have been isolated and characterized in animal and plants (Welters, 1996; Lemmon and Traub, 2000). However, limited information is available on the functions of *VPS* homologs in filamentous fungi, excluding *Aspergillus nidulans*, *A. oryzae* (Tarutani *et al.*, 2001; Ohsumi *et al.*, 2002; Oka *et al.*, 2004; Ohneda *et al.*, 2005), and *Magnaporthe oryzae* (Park and Lee, 2013). In this study, we describe the functions of a putative VPS encoding gene (*FgVPS74*) in the filamentous ascomycetous fungus, *Fusarium graminearum*, which was originally identified during the characterization of restriction enzyme-mediated integration (REMI) mutants of *F. graminearum* defective in hyphal growth and sexual development. *FgVPS74* is highly conserved across a wide range of filamentous fungi and is similar to the yeast *VPS74* gene (Bonangelino *et al.*, 2002) that plays a major role in the localization of a subset of Golgi enzymes (e.g., glycosyltransferase) by directly interacting with these enzymes (Schmitz *et al.*, 2008). However, the role of *VPS74*-like genes in filamentous fungi including *F. graminearum*, an important cereal pathogen, remain unclear (McMullen *et al.*, 1997). In the present study, we characterized the functions, expression, and localization of FgVPS74. Phenotypic changes caused by the deletion of *FgVPS74* in major mycological traits and cellular morphology in *F. graminearum* indicate the multiple roles of this key player in fungal physiology

Materials and Methods

Fungal strains, cultures, and outcross

The wild-type (WT) *F. graminearum* Z3643 strain used in this study is self-fertile and belongs to lineage 7 (*F. graminea-*

*For correspondence. E-mail: sy14@sch.ac.kr; Tel.: +82-41-5301288; Fax: +82-41-5303085

rum sensu stricto) of the *F. graminearum* species complex (O'Donnell *et al.*, 2000; Kim *et al.*, 2011). *F. graminearum* FLTRI6 has been developed as a reporter strain for trichothecene production using luminescence signals (Kim *et al.*, 2013), and FLTRI6ΔMAT2, derived from FLTRI6, is a self-sterile strain lacking *MAT1-2-1* (unpublished data). The R7048 strain is an insertional mutant derived from Z3643 through a REMI procedure using pIGPAPA DNA digested with *Kpn*I (Seo *et al.*, 2007). Fungal strains from 25% glycerol stock cultures stored at –80°C were maintained on complete medium (CM) (Leslie and Summerell, 2006), which was also used for vegetative growth. For conidiation, the strains were grown in either YMA medium (Semighini *et al.*, 2008) or CMC liquid medium (1.5% carboxymethyl cellulose, 0.1% yeast extract, 0.05% $MgSO_4 \cdot 7H_2O$, 0.1% NH_4NO_3, 0.1% KH_2PO_4). To induce sexual development, fungal strains were grown on carrot agar plates (Leslie and Summerell, 2006), as described previously (Kim *et al.*, 2008). For trichothecene production, fungal conidia were inoculated into minimal medium amended with agmatine at a final concentration of 1×10^4 /ml and incubated as described previously (Gardiner *et al.*, 2009). For an outcross, the conidial suspension of a male parent was dropped into the mycelial mat of the FLTRI6ΔMAT2 strain (female) that had previously been grown on carrot agar for 1 week, as described previously (Lee *et al.*, 2003).

Nucleic acid manipulations, plasmid rescue, sequencing, and PCR primers

General procedures for extraction of fungal genomic DNA (Chi *et al.*, 2009), restriction endonuclease digestion, agarose gel electrophoresis, gel blotting, ^{32}P probe labeling, and hybridization were performed as described previously (Sambrook and Russell, 2001). A plasmid rescue procedure was used to recover the DNA regions flanking the vector insertion site in the R7048 genome, as described previously (Yun *et al.*, 1998). Sequencing of the rescued plasmids was initiated with primers close to the *Kpn*I site on the pIGPAPA vector: pIGPAPA/P5 (5′-GGTCCCCCTCCCAATTCCTTTTC-3′) and TSP3-2 (5′-GCTCCTCGCCCTTGCTCACCAT-3′). The polymerase chain reaction (PCR) primers (Table 1) used in this study were synthesized by the Bioneer oligonucleotide synthesis facility (Bioneer), dissolved (100 μM) in sterilized water, and stored at -20°C.

Vector construction

A fungal transforming DNA construct for targeted gene deletion was created using the double-joint PCR method, as described previously (Yu *et al.*, 2004; Lee *et al.*, 2009). DNA fragments corresponding to the 5′ and 3′ flanking regions of the *FgVPS74* ORF were amplified from genomic DNA of Z3643 using the VPS5F / VPS5Rt and VPS3Ft / VPS3R primer pairs (Table 1), respectively, and mixed with the hygromycin B (hygB) resistant gene (hygromycin phosphotransferase, designated *hph*) cassette amplified with primers hygB-5for and hygB-3rev (Table 1) from the vector pBCATPH. A second round of PCR using the nested VPS5N and VPS3N primer pair (Table 1) resulted in a 4.5-kb fragment of the final fusion PCR product. For GFP-tagging of the *FgVPS74* construct, a plasmid DNA carrying the *GFP* gene fused with the 5′ end of the *FgVPS74* ORF, which was under control of its native promoter region (4.5 kb) (Pnative-*GFP-FgVPS74*), was generated using a double-joint PCR approach (Yu *et al.*, 2004). To accomplish this, three targets were amplified from pCHPH1 (Kwon *et al.*, 2009), pIGPAPA (Lee *et al.*, 2003), and Z3643 with the primer pairs VPS3R / VPSGFP-3Ft, GFP_for/GFP_rev, and VPS5F / VPSGFP-5Rt, respectively, mixed in a 1:1:3 molar ratio, and finally fused together using the nested primer set VPS3N and VPS5N. The final PCR product was inserted into the pGEMT vector (Promega).

Fungal transformation, virulence test, and luminescence assay

The fusion PCR product alone or in combination with the pBCATPH vector carrying *hph* was added to the protoplasts of the Z3643 or *FgVPS34*-deletion (Δ*FgVPS74*) strains, as described previously (Kim *et al.*, 2008, 2011). Virulence of the fungal strains was determined on spikelets of wheat, as described previously (Kim *et al.*, 2013). Luciferase activity in cell lysates from fungal strains was measured using GloMax® 96 Microplate Luminometer (Promega), as described previously (Kim *et al.*, 2012).

Electron microscopy and other microscopic observations

For scanning electron microscopy, agar blocks (5×5 mm^2) containing hyphae of each specimen (Z3643, Δ*FgVPS74*, and CoVPS74) were immersed in a modified Karnovsky's fixative consisting of 2% (v/v) glutaraldehyde and 2% (v/v) paraformaldehyde in 0.05 M sodium cacodylate buffer, as

Table 1. Primers used in this study

Name	Nucleotide sequence (5′–3′)	Amplified region
VPS5F	TCGACGAGAATGCCAGCAACTTTACCT	5′ flank of *FgVSP74*
VPS5Rt	TGACCTCCACTAGCTCCAGCCAAGCAAACACGATGCCTGGATTAC	
VPS3Ft	TATGAAAATTCCGTCACCAGCCGATATGTTTTGTCTTTGGTGT	3′ flank of *FgVSP74*
VPS3R	GCTTAAGCTGCATCTGCCTCCTGTG	
VPS5N	GCAAAAAGGAGAAGAAGCATGAGAAGGATT	
VPS3N	GCTTAAGCTGCATCTGCCTCCTGTG	
VPSGFP-5Rt	CTCACGGCATGGACGAGCTGTACAAGTCCTCGGGATTGACGCGACGCCGC	
VPSGFP-3Ft	AACAGCTCCTCGCCCTTGCTCACCATTTCGAAGAGGTAGATATGTTTTGT	
GFP for	ATGGTGAGCAAGGGCGAGGAGCTGT	*GFP*
GFP rev	CTTGTACAGCTCGTCCATGCCGTGAG	
hygB-5for	CTTGGCTGGAGCTAGTGGAGGT	*hygB*
hygB-3rev	GGCTGGTGACGGAATTTTCA	

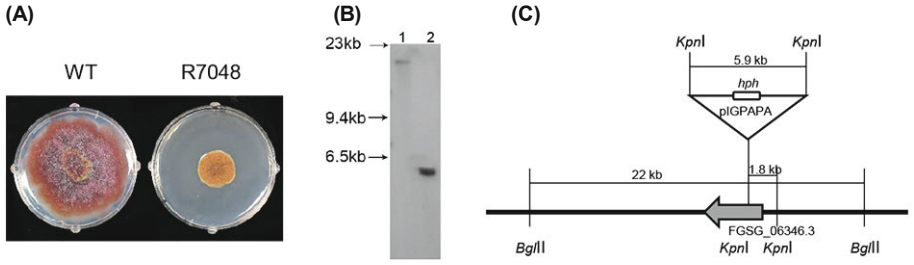

Fig. 1. Phenotypic changes and molecular analysis of the vector insertions in the REMI mutant R7048 of *F. graminearum*. (A) Hyphal growth on CM. (B) DNA gel blot of R7048 digested with *Bgl*II (lane 1) and *Kpn*I (lane 2), probed with pIGPAPA. The size markers of lambda DNA standards are indicated to the left of the blot. (C) Molecular structure of vector insertion site in the genome of R7048. The ORF within the vector insertion site is indicated by the filled arrow.

described previously (Kim, 2008). Briefly, the specimens were washed with the same buffer, post-fixed with 1% (w/v) osmium tetroxide in the same buffer, and washed with distilled water. The post-fixed specimens were dehydrated in a graded ethanol series, treated with isoamyl acetate, and dried in a critical point drier (CPD 030, BAL-TEC). They were then mounted on metal stubs and coated with platinum using a sputter-coater (SCD 005, BAL-TEC). The specimens were examined with a field emission scanning electron microscope (Supra 55VP, Carl Zeiss) at 2 kV.

For transmission electron microscopy, agar blocks (1 × 3 mm^2) containing fungal hyphae were fixed and further processed, as described previously (Kim, 2008). Briefly, the post-fixed specimens were *en bloc* stained with 0.5% uranyl acetate, dehydrated in a graded ethanol series, and embedded in Spurr's resin. Ultrathin sections (60 nm thick) were generated with a diamond knife using an ultramicrotome (MT-X, RMC). The sections were mounted on copper grids and stained with 2% uranyl acetate and Reynolds' lead citrate. The specimens were examined with a transmission electron microscope (JEM-1010, JEOL) at 80 kV.

Differential interference contrast (DIC) microscopic observations were performed using an image analysis system consisting of a microscope (Leica DM 2000) with an attached digital camera (Leica DFC 550) and a computer. Vacuole shapes in vegetative hyphae were observed by staining with neutral red, as described previously (Park and Lee, 2013).

Results

Phenotypes and molecular characterization of the REMI mutant R7048

An insertional mutant of *F. graminearum*, designated R7048, was initially selected from the previously generated REMI mutant collection (Seo *et al.*, 2007). Compared with its WT progenitor Z3643, the mutant R7048 showed significant reduction (~70% less than WT) in radial growth with fewer aerial mycelia and less pigmentation on PDA or CM (Fig. 1A). After removing the aerial mycelia for perithecial induction on carrot agar, R7048 formed no sexual fruiting

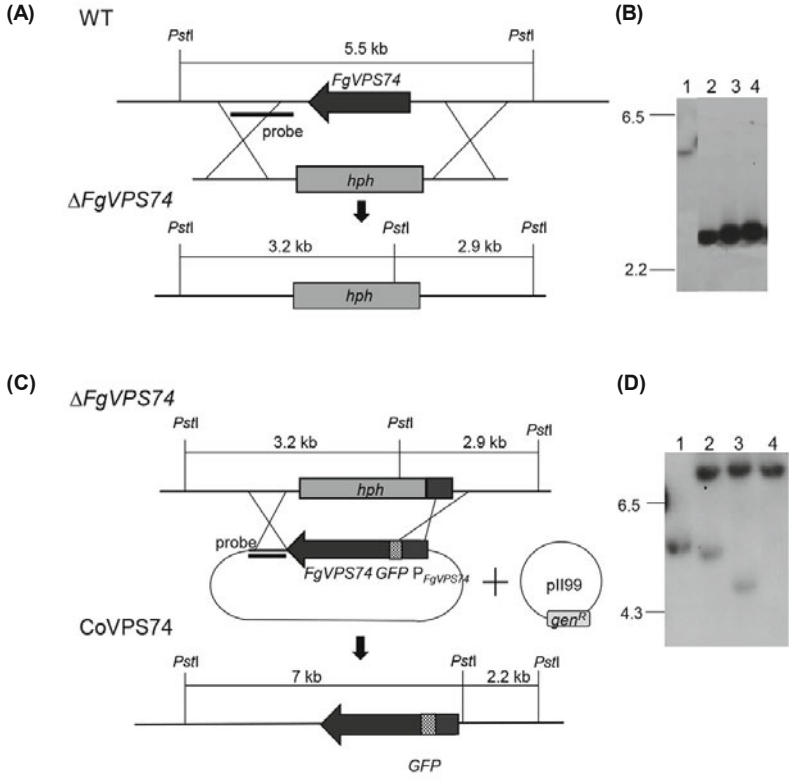

Fig. 2. Targeted gene deletion of *FgVPS74* from the genome of *F. graminearum* Z3643 and complementation analyses. (A) Deletion scheme. WT: genomic DNA of Z3643, Δ*FgVPS74*: the Z3643 strain carrying the deletion of *FgVPS74*. (B) DNA gel blot of the WT and Δ*FgVPS74* strains digested with *Pst*I, hybridized with a 3′ flanking region of the *FgVPS74* ORF. Lanes: 1, WT; 2–4; the Δ*FgVPS74* strains, (C) Complementation by the co-transformation strategy using circular pII99 DNA. CoVPS74: the Δ*FgVPS74* strain carrying a functional GFP-tagged *FgVPS74* copy. $P_{FgVPS74}$: a putative promoter region of *FgVPS74*. (D) DNA gel blot of the complemented strains, hybridized with the 3′ flanking region of the *FgVPS74* ORF. Lanes: 1, WT; 2–4, complemented strain. The strain of lane 4 was selected as a complemented strain (CoVPS74) for further use.

bodies (perithecia) within 6 weeks, whereas Z3643 began to produce fertile perithecia 5 days after perithecial induction. In addition, R7048 produced no trichothecene in agmatine liquid medium and showed reduced virulence on wheat (data not shown).

To characterize the vector insertion in the R7048 genome, a gel blot of R7048 genomic DNA was hybridized with the REMI vector, pIGPAPA, as a probe. A single vector size (5.9 kb) hybridizing fragment was observed in the genomic DNA digested with *Kpn*I, which was the enzyme used for vector linearization in the REMI procedure, suggesting that a single copy of the vector integrated at a *Kpn*I site in the fungal genome (Fig. 1B). Furthermore, a single 22.0-kb hybridizing band appeared in the genomic DNA digested with *Bgl*II (which had no recognition site in pIGPAPA) and confirmed single vector integration in the fungal genome (Fig. 1B). Nucleotide sequencing of the 22.0-kb *Bgl*II fragment, recovered using a plasmid rescue procedure, revealed that it contained 4.3 kb of genomic DNA to the left side and 11.8 kb to the right side of the vector. BLAST search of the *F. graminearum* genome database (http://www.broadinstitute.org/annotation/genome/fusarium_group/MultiHome.html) revealed that the REMI vector disrupted a 1,252-bp gene, designated *FgVPS74* (annotated as FGSG_06346), showing similarity to vacuolar protein sorting-associated protein 74 (Fig. 1C).

Targeted deletion of *FgVPS74* and complementation

To confirm that disruption of *FgVPS74* is the direct cause of the pleiotropic changes in R7048, the genomic copy of *FgVPS74* was deleted from the genome of the WT Z3643 strain using a targeted gene deletion strategy (Fig. 2A). Replacement of the *FgVPS74* ORF with a *hph* gene cassette via double homologous recombination resulted in deletion of *FgVPS74* (designated Δ*FgVPS74*), as confirmed by DNA gel blot hybridization (Fig. 2B). *Pst*I-digested genomic DNA of the Δ*FgVPS74* strains showed a single 3.2-kb hybridizing band instead of the 5.5-kb band found in Z3643, confirming that the entire 1.2-kb of *FgVPS74* ORF had been replaced by *hph*. To confirm the function of *FgVPS74* in *F. graminearum*, an intact copy of *FgVPS74* fused to GFP (the Pnative-*GFP-FgVPS74* construct described in the 'Materials and Methods' section) was introduced into the genome of a Δ*FgVPS74* strain. The plasmid carrying the 4.5-kb *GFP-gVPS74* DNA fragment was directly added to protoplasts of the Δ*FgVPS74* strain, along with pII99 carrying the geneticin resistance gene (*genR*) as a fungal selectable marker (Fig. 2C). The geneticin-resistant transformants that were no longer resistant to hygromycin B were selected as genetically complemented (or add-back) strains. DNA gel blot analysis confirmed insertion of the *GFP-FgVPS74* construct at its original genomic locus of the recipient Δ*FgVPS74* strain, leading to the loss of *hph* in the complements (Fig. 2C and D).

Defects in hyphal growth, conidiation, and sexual development in the Δ*FgVPS74* strain

All Δ*FgVPS74* strains showed the same pleiotropic phenotypes as the original REMI mutant, R7048. Radial growth of the Δ*FgVPS74* strains was significantly reduced compared to the untransformed WT progenitor Z3643 under several growth conditions. The Δ*FgVPS74* strains produced fewer aerial mycelia and more yellowish or white mycelia on PDA and carrot agar, respectively, which appeared denser than those of Z3643 (Fig. 3A). In addition, the Δ*FgVPS74* strains showed severe alterations in conidial production and morphology. The number and length of conidia produced by the Δ*FgVPS74* strain, determined in CMC liquid medium and on YMA, were approximately 0.03% and 70% of the WT levels, respectively (Fig. 3B and C). Self-crossing of the Δ*FgVPS74* strain produced no perithecia on carrot agar (Fig. 3D), whereas outcrossing to the FLTRI6ΔMAT2 as a female parent produced fertile perithecia carrying normal ascospore-bearing asci (data not shown), which suggested that the Δ*FgVPS74* strain retained the ability to outcross as a male. These severe defects in fungal traits were restored to the wild-type levels when a native copy of *FgVPS74* was introduced into the gene deletion strain (Fig. 3).

Defects in virulence and mycotoxin production in the Δ*FgVPS74* strain

In virulence tests, the WT and complemented (add-back) strains examined caused typical head blight and complete

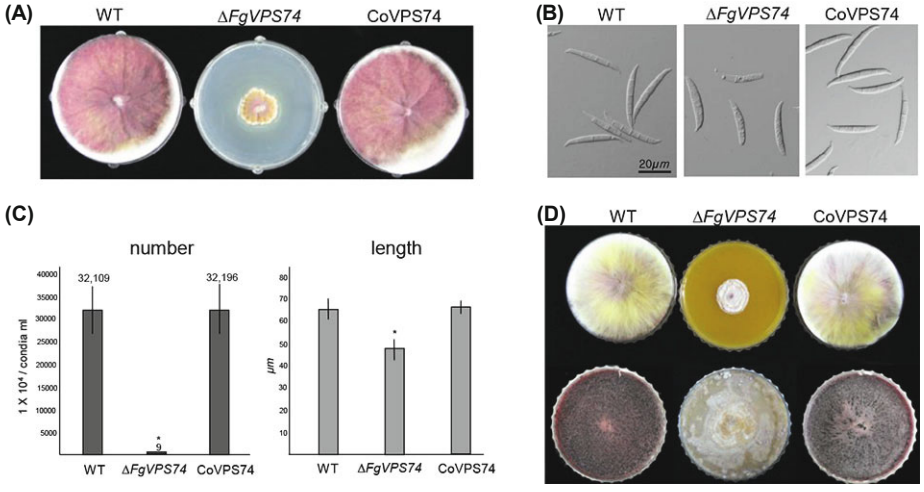

Fig. 3. Phenotypes of the Δ*FgVPS74* strain. (A) Hyphal growth on CM. (B) Conidial morphology on YMA medium. (C) Conidial production in CMC liquid medium (for conidial number) or on YMA medium (for conidial length). The experiment was performed with three independent replicates and error bars represent standard errors. Tukey's test was performed to examine the significant differences ($P < 0.05$) among the mean values of the samples. (D) Perithecia formation on carrot agar.

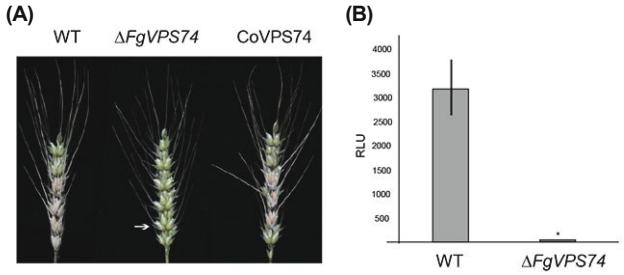

Fig. 4. Virulence of the Z3643 (WT), Δ*FgVPS74*, and CoVPS74 strains on wheat heads (A), and *Tri6* expression levels in the WT and Δ*FgVPS74* strain, determined based on the luminescence signal for *Tri6* gene expression (B). The injection point for inoculation is indicated by an arrow. RLU: relative luminescence units. Data obtained from three replicates. Error bars represent standard errors.

bleaching on wheat. However, the Δ*FgVPS74* strains caused few blight symptoms even on the inoculated spikelets (Fig. 4A). The effect of *FgVPS74* deletion on the production of trichothecenes in *F. graminearum* was determined using the luminescent reporter strain (FLTRI6) derived from Z3643, which carries the fruit fly luciferase gene under control of the *Tri6* promoter encoding a transcription factor required for trichothecene biosynthesis (Kim *et al.*, 2013). The Δ*FgVPS74* strain in the genetic background of FLTRI6 (designated Δ*FgVPS74*-FLTRI6) was selected among progeny from an outcross between Δ*FgVPS74* and FLTRI6ΔMAT2 strains. Luminescence signal intensity from cell lysates extracted from the Δ*FgVPS74*-FLTRI6 strains examined, which were grown in AG medium for 6 days, decreased at least 3,000-fold compared to those from the FLTRI6 strain, indicating that trichothecene biosynthesis was severely affected by Δ*FgVPS74*. (Fig. 4B).

Microscopic observation and cellular localization of FgVPS74

Field emission scanning electron microscopy revealed normal hyphal growth of the wild-type Z3643 strain. The hyphae were approximately 5 μm in diameter and showed massive branching and elongation (Fig. 5A). Transmission electron microscopy revealed normal eukaryotic cytoplasm containing mitochondria and endoplasmic reticula (Fig. 5B). However,

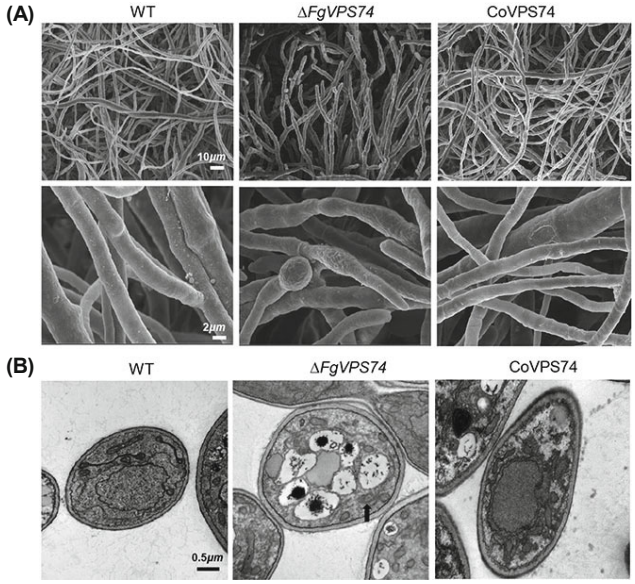

Fig. 5. Electron microscopic observation of hyphae in the WT, Δ*FgVPS74*, and CoVPS74 strains. (A) Scanning electron microscopic observation, (B) transmission electron microscopic observation. A mitochondrion is indicated by an arrow.

the hyphae of the Δ*FgVPS74* strain were characterized by limited branching and elongation. Higher magnifications revealed a balloon-shaped terminal or intercalary hyphal swelling (Fig. 5A). In addition, aberrant increase in mitochondrial number was prominent in the Δ*FgVPS74* strain (Fig. 5B). Meanwhile, an evident morphological difference in hyphal growth was not observed between the wild-type and CoVPS74 strains. It was common to observe the proliferation of hyphal branching and elongation. The hyphae appeared to possess normal cytoplasm filled with mitochondria and lipid globules. Vacuole staining with natural red showed no significant differences in size and morphology between Z3643 or CoVPS74 strain and Δ*FgVPS74* strain. Most vacuoles observed in the strains examined were circular types (Fig. 6A). The expression of GFP-tagged FgVPS74 and its sub-cellular localization were visualized using the CoVPS74 strain via

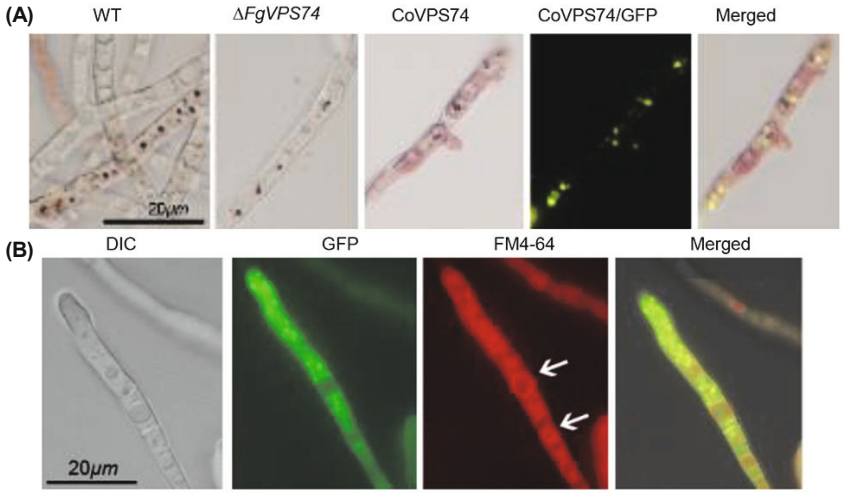

Fig. 6. Observation of hyphal vacuoles in the WT, Δ*FgVPS74*, and CoVPS74 strains. (A) DIC observation of vacuoles stained with natural red in the WT, Δ*FgVPS74*, and CoVPS74 strains (in first three panels), GFP imaging of the CoVPS74 strain under a fluorescence microscope (in the fourth panel), and a merged image of the CoVPS74 strain (in the fifth panel). (B) DIC and fluorescence microscopic observations of hyphae in the CoVPS74 strain stained with FM4-64. The vacuolar membrane ring pattern is indicated by an arrow.

fluorescence microscopy. Complete restoration of the phenotypic defects caused by Δ*FgVPS74* in the CoVPS74 strain indicated that the GFP signal from GFP-tagged FgVPS74 in this strain should reflect the native localization of the FgVPS74 protein since this GFP-tagged construct did not affect the function of FgVPS74. In young mycelia, the GFP signal of FgVPS74 was detectable throughout the majority of the cytoplasm (Fig. 6B), but in aging mycelia it was specifically localized to vesicle-like structures (likely endosomes in the trans-Golgi network) (Fig. 6A). Interestingly, GFP-FgVPS74 did not localize to the vacuolar membranes that were shown as a ring staining pattern when stained with FM4-64, as seen in *S. cerevisiae* (Fig. 6B) (Vida and Emr, 1995). Similarly, the GFP signal was not co-localized with the vacuoles stained with natural red (Fig. 6A).

Discussion

The yeast Vps74 protein is a novel hypothetical protein that interacts with Vps26p, a component of the Vps5p-Vps17p-Vps26p-Vps29p-Vps35p retromer complex that is localized to endosomal membranes and required for endosome-to-Golgi retrieval of the vacuolar hydrolase receptor, Vps10p (Bonangelino *et al.*, 2002; Bonifacino and Rojas, 2006). Vps74p mediates the predominant localization of a subset of Golgi enzymes (e.g., glycosyltransferase) to early (*cis* and *medial*) Golgi compartments by directly binding to the cytosolic domains of these enzymes (Schmitz *et al.*, 2008). In yeast cells, loss of Vps74 function leads to degradation of Golgi enzymes in the lysosome-like vacuole and severe glycosylation defects of secretory cargo (Schmitz *et al.*, 2008; Tu *et al.*, 2008; Wood *et al.*, 2009), as well as perturbation of complex sphingolipid homeostasis (Wood *et al.*, 2012). In addition, defects in the localization of glycosyltransferases cause a number of congenital disorders of glycosylation (CDG) diseases in human (Jaeken and Matthijs, 2007). In contrast to the cases of yeast, little is known regarding the functions of *VPS74* in the physiology of filamentous fungi, with the exception of the rice blast fungus *M. oryzae* where the phenotypic changes caused by the disruption of a putative promoter region of a *VPS74*-like gene (*MoVPS74*) were described briefly (Park and Lee, 2013). Along with the *M. oryzae* mutant (designated MoVPS74^{BiG}), the availability of the *F. graminearum* lacking *FgVPS74*, an orthologue of the yeast *VPS74,* in this study allows us to explore how the proper localization of Golgi enzymes affects several traits in filamentous fungi. Localization of a GFP-FgVPS74 fusion construct to possible endosome structures, but not to the vacuolar membrane, indicates that FgVPS74 may be a functional homologue of the yeast Vps74p in *F. graminearum* because it binds directly to proteins residing in the Golgi compartments.

The most common phenotypes in the *VPS74* mutants from the two fungal species were strikingly reduced hyphal growth and fungal virulence on host plants. The possible defects in protein trafficking and sorting pathways in these mutants may be the direct cause of these pleiotropic changes since hyphal growth in filamentous fungi requires many matrix components that are typically delivered by vesicle trafficking (Wessels, 1990; Gupta and Heath, 2002). Additionally, both mutants showed abnormal hyphal morphology with swollen hyphal tips confirmed by light microscope and SEM observations, which is also similar to the phenotype of impaired cell wall shown in the *F. graminearum* strain lacking a mitogen-activated protein kinase gene (*MGV1*) (Hou *et al.*, 2002), indicating that *FgVPS74* may be required for maintain cell wall integrity.

The altered virulence of two mutant strains on host plants (rice or wheat) may be associated with defects in hyphal growth and/or proper delivery of some proteins through the vacuolar-sorting pathway, which may be important in fungal virulence. However, the quantitative effect of the *VPS74* gene disruption on virulence varied among these two plant pathogenic fungi, which have different infection mechanisms: one is hemibiotrophic and the other is necrotrophic. The *M. oryzae* MoVPS74^{BiG} strain retains the ability to form lesions on rice leaves, while the *F. graminearum* Δ*FgVPS74* strain caused almost no disease symptoms in wheat head. The capacity of the former to cause disease symptoms could be attributed to its ability for normal appressorium formation and conidial germination (Park and Lee, 2013). In contrast, the abolishment of virulence in the latter may be caused by its additive defects in production of the trichothecene mycotoxin, which is known to be a virulence factor in *F. graminearum* (Proctor *et al.*, 1995), and in conidial production, along with its retarded hyphal growth. Self-sterility of the Δ*FgVPS74* strain could also be attributed to the pleiotropic defects in hyphal growth and conidiation, which had not been explored in *M. oryzae*. The other prominent phenotype caused by Δ*FgVPS74* is the increase in the number of mitochondria, which has been not observed in various *VPS* mutants of *S. cerevisiae*, although disruption of class C *VPS* genes resulted in mitochondrial defects (Wang and Deschenes, 2006). This suggests that Δ*FgVPS74* leads to metabolic defects in *F. graminearum*, which should be counterbalanced by the increased mitochondrial mass. However, further investigations are required to confirm this hypothesis.

In conclusion, functional investigations of *FgVPS74* presented in this study confirm that the proper vacuolar sorting pathway, particularly the localization of Golgi-resident proteins, is a fundamental and conserved process for several traits such as hyphal growth, conidiation, sexual development, virulence, and mycotoxin production in the cereal pathogen, *F. graminearum*.

Acknowledgements

This work was supported by the Soonchunhyang University Research Fund (NO: 20120721).

References

Bonangelino, C.J., Chavez, E.M., and Bonifacino, J.S. 2002. Genomic screen for vacuolar protein sorting genes in *Saccharomyces cerevisiae*. *Mol. Biol. Cell.* **13**, 2486–2501.

Bonifacino, J.S. and Rojas, R. 2006. Retrograde transport from endosomes to the trans-Golgi network. *Nat. Rev. Mol. Cell Biol.* **7**, 568–579.

Chi, M.H., Park, S.Y., and Lee, Y.H. 2009. A quick and safe method

for fungal DNA extraction. *Plant Pathol. J.* **25**, 108–111.
Conibear, E. and Stevens, T.H. 1995. Vacuolar biogenesis in yeast: sorting out the sorting proteins. *Cell* **83**, 513–516.
Gardiner, D.M., Kazan, K., and Manners, J.M. 2009. Novel genes of *Fusarium graminearum* that negatively regulate deoxynivalenol production and virulence. *Mol. Plant-Microbe Interact.* **22**, 1588–1600.
Gupta, G.D. and Heath, I.B. 2000. A tip-high gradient of a putative plasma membrane SNARE approximates the exocytotic gradient in hyphal apices of the fungus *Neurospora crassa*. *Fungal Genet. Biol.* **29**, 187–199.
Hou, Z., Xue, C., Peng, Y., Katan, T., Kistler, H.C., and Xu, J.R. 2002. A mitogen-activated protein kinase gene (*MGV1*) in *Fusarium graminearum* is required for female fertility, heterokaryon formation, and plant infection. *Mol. Plant-Microbe Interact.* **15**, 1119–1127.
Jaeken, J. and Matthijs, G. 2007. Congenital disorders of glycosylation: a rapidly expanding disease family. *Annu. Rev. Genomics Hum. Genet.* **8**, 261–278.
Kim, H.K., Cho, E.J., Jo, S., Sung, B.R., Lee, S., and Yun, S.H. 2012. A split luciferase complementation assay for studying *in vivo* protein-protein interactions in filamentous ascomycetes. *Curr. Genet.* **58**, 179–189.
Kim, H.K., Lee, S., Jo, S.M., McCormick, S.P., Butchko, R.A., Proctor, R.H., and Yun, S.H. 2013. Functional roles of FgLaeA in controlling secondary metabolism, sexual development, and virulence in *Fusarium graminearum*. *PLoS One* **8,** e68441.
Kim, H.K., Lee, T., and Yun, S.H. 2008. A putative pheromone signaling pathway is dispensable for self-fertility in the homothallic ascomycete *Gibberella zeae*. *Fungal Genet. Biol.* **45**, 1188–1196.
Kim, H.K., Lee, Y.W., and Yun, S.H. 2011. *GzRUM1,* encoding an ortholog of human retinoblastoma binding protein 2, is required for ascospore development in *Gibberella zeae*. *Plant Pathol. J.* **27**, 20–25.
Kim, K.W. 2008. Visualization of micromorphology of leaf epicuticular wax of the rubber tree *Ficus elastica* by electron microscopy. *Micron.* **39**, 976–984.
Kwon, B.R., Kim, M.J., Park, J.A., Chung, H.J., Kim, J.M., Park, S.M., Yun, S.H., Yang, M.S., and Kim, D.H. 2009. Assessment of the core cryparin promoter from *Cryphonectria parasitica* for heterologous expression in filamentous fungi. *Appl. Microbiol. Biotechnol.* **83**, 339–348.
Lee, S.H., Han, Y.K., Yun, S.H., and Lee, Y.W. 2009. Roles of the glyoxylate and methylcitrate cycles in sexual development and virulence in the cereal pathogen *Gibberella zeae*. *Eukary. Cell.* **8**, 1155–1164.
Lee, J., Lee, T., Lee, Y.W., Yun, S.H., and Turgeon, B.G. 2003. Shifting fungal reproductive mode by manipulation of mating type genes: obligatory heterothallism of *Gibberella zeae*. *Mol. Microbiol.* **50**, 145–152.
Lemmon, S.K. and Traub, L.M. 2000. Sorting in the endosomal system in yeast and animal cells. *Curr. Opin. Cell Biol.* **12**, 457–466.
Leslie, J.F. and Summerell, B.A. 2006. The Fusarium lab manual, Blackwell, Ames, IA, USA.
McMullen, M., Jones, R., and Gallenberg, D. 1997. Scab of wheat and barley: a re-emerging disease of devastating impact. *Plant Dis.* **81**, 1340–1348.
O'Donnell, K., Kistler, H.C., Tacke, B.K., and Casper, H.H. 2000. Gene genealogies reveal global phylogeographic structure and reproductive isolation among lineages of *Fusarium graminearum*, the fungus causing wheat scab. *Proc. Natl. Acad. Sci. USA* **97**, 7905–7910.
Ohneda, M., Arioka, M., and Kitamoto, K. 2005. Isolation and characterization of *Aspergillus oryzae* vacuolar protein sorting mutants. *Appl. Environ. Microbiol.* **71**, 4856–4861.
Ohsumi, K., Arioka, M., Nakajima, H., and Kitamoto, K. 2002. Cloning and characterization of a gene (*avaA*) from *Aspergillus nidulans* encoding a small GTPase involved in vacuolar biogenesis. *Gene* **291**, 77–84.
Oka, M., Maruyama, J., Arioka, M., Nakajima, H., and Kitamoto, K. 2004. Molecular cloning and functional characterization of *avaB*, a gene encoding Vam6p/Vps39p-like protein in *Aspergillus nidulans*. *FEMS Microbiol. Lett.* **232**, 113–121.
Park, J. and Lee, Y.H. 2013. Bidirectional-genetics platform, a dual-purpose mutagenesis strategy for filamentous fungi. *Eukary. Cell* **12**, 1547–1553.
Proctor, R.H., Hohn, T.M., and McCormick, S.P. 1995. Reduced virulence of *Gibberella zeae* caused by disruption of a trichothecene toxin biosynthetic gene. *Mol. Plant-Microbe Interact.* **8**, 593–601.
Raymond, C.K., Howald-Stevenson, I., Vater, C.A., and Stevens, T.H. 1992. Morphological classification of the yeast vacuolar protein sorting mutants: evidence for a prevacuolar compartment in class E vps mutants. *Mol. Biol. Cell* **3**, 1389–1402.
Robinson, J.S., Klionsky, D.J., Banta, L.M., and Emr, S.D. 1988. Protein sorting in *Saccharomyces cerevisiae*: isolation of mutants defective in the delivery and processing of multiple vacuolar hydrolases. *Mol. Cell. Biol.* **8**, 4936–4948.
Rothman, J.H., Howald, I., and Stevens, T.H. 1989. Characterization of genes required for protein sorting and vacuolar function in the yeast *Saccharomyces cerevisiae*. *EMBO J.* **8**, 2057–2065.
Sambrook, J. and Russell, D.W. 2001. Molecular cloning: a laboratory manual, Cold Spring Harbor Laboratory Press, Plainview, USA.
Schmitz, K.R., Liu, J., Li, S., Setty, T.G., Wood, C.S., Burd, C.G., and Ferguson, K.M. 2008. Golgi localization of glycosyltransferases requires a Vps74p oligomer. *Develop. Cell* **14**, 523–534.
Semighini, C.P., Murray, N., and Harris, S.D. 2008. Inhibition of *Fusarium graminearum* growth and development by farnesol. *FEMS Microbiol. Lett.* **279**, 259–264.
Seo, B.K., Kim, H.K., Lee, Y.W., and Yun, S.H. 2007. Functional analysis of a histidine auxotrophic mutation in *Gibberella zeae*. *Plant Pathol. J.* **23**, 51–56.
Tarutani, Y., Ohsumi, K., Arioka, M., Nakajima, H., and Kitamoto, K. 2001. Cloning and characterization of *Aspergillus nidulans vpsA* gene which is involved in vacuolar biogenesis. *Gene* **268**, 23–30.
Tu, L., Tai, W.C., Chen, L., and Banfield, D.K. 2008. Signal-mediated dynamic retention of glycosyltransferases in the Golgi. *Science* **321**, 404–407.
Veses, V., Richards, A., and Gow, N.A. 2008. Vacuoles and fungal biology. *Curr. Opin. Microbiol.* **11**, 503–510.
Vida, T.A. and Emr, S.D. 1995. A new vital stain for visualizing vacuolar membrane dynamics and endocytosis in yeast. *J. Cell Biol.* **128**, 779–792.
Wang, G. and Deschenes, R.J. 2006. Plasma membrane localization of Ras requires class C Vps proteins and functional mitochondria in *Saccharomyces cerevisiae*. *Mol. Cell. Biol.* **26**, 3243–3255.
Wessels, J.G.H. 1990. Role of cell wall architecture in fungal tip growth generation, pp. 1–29. *In* Heath, I.B. (ed.), Tip Growth in Plant and Fungal Cells, Academic Press, San Diego, USA.
Welters, P. 1996. Vacuolar targeting: proteins of the transport machinery. *Plant Physiol. Biochem.* **34**, 229–235.
Wood, C.S., Hung, C.S., Huoh, Y.S., Mousley, C.J., Stefan, C.J., Bankaitis, V., Ferguson, K.M., and Burd, C.G. 2012. Local control of phosphatidylinositol 4-phosphate signaling in the Golgi apparatus by Vps74 and Sac1 phosphoinositide phosphatase. *Mol. Biol. Cell* **23**, 2527–2536.
Wood, C.S., Schmitz, K.R., Bessman, N.J., Setty, T.G., Ferguson, K.M., and Burd, C.G. 2009. PtdIns4P recognition by Vps74/GOLPH3 links PtdIns 4-kinase signaling to retrograde Golgi trafficking. *J. Cell Biol.* **187**, 967–975.
Yu, J.H., Hamari, Z., Han, K.H., Seo, J.A., Reyes-Dominguez, Y., and Scazzocchio, C. 2004. Double-joint PCR: a PCR-based molecular tool for gene manipulations in filamentous fungi. *Fungal Genet. Biol.* **41**, 973–981.
Yun, S.H., Turgeon, B.G., and Yoder, O.C. 1998. REMI-induced mutants of *Mycosphaerella zeae-maydis* lacking the polyketide PM-toxin are deficient in pathogenesis to corn. *Physiol. Mol. Plant Pathol.* **52**, 53–66.